DEVELOPING SITE-SPECIFIC VERTICAL GROUND MOTIONS FOR TURKEY PART 1: USING V/H RATIO GROUND MOTION MODELS

Z. GÜLERCE[1], N. A.ALIPOUR[1], M. A. SANDIKKAYA[2]

[1] Middle East Technical University, Ankara, Turkey

[2] Hacettepe University, Ankara, Turkey

E-mail contact of main author: zyilmaz@metu.edu.tr

Abstract. Ongoing feasibility and site licensing studies for the Akkuyu and Sinop Nuclear Power Plant sites underlined the need for the guidelines of estimating the vertical design spectrum in the Probabilistic Seismic Hazard Assessment (PSHA) studies conducted in Turkey. For this purpose, the Turkish Strong Motion Database (TSMD) (Akkar et al., 2010; Gulerce et al., 2016) is updated with the recordings from the earthquakes occurred between 2008 and 2015, including the M_w=6.1 Elazığ and M_w=7.2 Van earthquakes. Updated strong motion database contains 2698 recordings with the earthquake metadata, source-to-site distance metrics for the recordings, measured V_{S30} values for the recording stations, and horizontal and vertical component spectral acceleration values. There are two main approaches that can be used to develop the vertical design spectra; computing the hazard for vertical ground motions using vertical ground motion models (GMMs) or using V/H ratio GMMs to scale the horizontal spectrum. Following the second approach, four candidate V/H ratio GMMs (proposed by Gulerce and Abrahamson, 2011; Gulerce and Akyuz, 2013; Akkar et al., 2014; Bozorgnia and Campbell, 2016) are selected and the model predictions are compared with the actual data in the updated dataset using the analysis of the residuals. Analysis results showed that the median predictions of the V/H ratio GMMs proposed by Gulerce and Akyuz (2013), Akkar et al., (2014) and Bozorgnia and Campbell (2016) are compatible with the V/H ratios in the Turkish strong motion dataset. Findings of this study and the ongoing compatibility analysis of the vertical GMMs with the updated dataset will be combined to provide a complete framework of ground motion characterization for vertical ground motion component in Turkey.

Key Words: Turkish Strong Motion Database, Ground motion models, Residual analysis, V/H ratio

1. INTRODUCTION

Strong ground motions recorded during the earthquakes occurred between 1976 and 2007 were gathered and compiled together with the relevant earthquake and site metadata as the Turkish Strong Ground Motion Database (TSMD) by Akkar et al. (2010) [1] and Sandıkkaya et al. (2010) [2]. In 2014, Akkar et al. (2014) [3] revisited the earthquake metadata of TSMD and added only the moderate-to-high magnitude earthquakes occurred after 2008 (e.g. 2010 Elazığ (M_w=6.2), 2011 Simav (M_w=5.9), 2011 Van (M_w=7.1) and Edremit (M_w=5.9) earthquakes) to TSMD within the context of Reference Database for Seismic Ground-Motion in Europe (RESORCE) which is a product of Seismic Ground Motion Assessment project (SIGMA; projet-sigma.com). Gulerce et al. (2016) [4] used the first version of TSMD to test the compatibility of the strong motions recorded in Turkey with the Next Generation Attenuation (NGA) West 1 ground motion models (GMMs). Incompatibilities between the NGA-W1 GMMs and Turkish strong motion dataset in small-to-moderate magnitude scaling, large distance scaling, and site amplification scaling were encountered during the evaluation of the residuals, indicating that the GMMs for the vertical ground motions or vertical to horizontal (V/H) ratio should be compared to the Turkish dataset for building a ground

motion characterization logic tree for vertical ground motion component. Ongoing feasibility and site licensing studies for the Akkuyu and Sinop Nuclear Power Plant sites clearly underlined the need for the guidelines of estimating the vertical design spectrum in the Probabilistic Seismic Hazard Assessment (PSHA) studies conducted in Turkey.

Between years 2008 and 2015, a considerable amount of strong motions recorded during low-to-moderate magnitude earthquakes in Turkey were accumulated. These recordings are available in AFAD's (The Disaster and Emergency Management Presidency of Turkey) Strong Motion Database of Turkey (http://kyhdata.deprem.gov.tr/2K/kyhdata_v4.php) but the provided waveforms are not processed nor are the earthquake metadata compiled for these recordings. One of the main goals of this study is to process these recordings in a manner that is consistent with TSMD effort and to extend the TSMD to cover the recordings until the end of 2015, both for the vertical and horizontal ground motion components. In 2017, an earthquake swarm was occurred in northwest Turkey (Ayvacık region of Çanakkale) providing a significant amount of recordings in low magnitude range. This data is also compiled and added to the updated TSMD. First part of this article presents the updated TSMD by providing statistical information about newly added recordings and describing the ground motion processing scheme. Updated TSMD is used to test the compatibility of the recent vertical and V/H ratio GMMs with the Turkish strong motion recordings. In this manuscript, the procedure followed to evaluate the compatibility of the estimations of candidate V/H ratio GMMs with observed data in terms of main seismological parameters (e.g., earthquake magnitude, style-of-faulting, depth to the top of rupture, distance, and site-amplification scaling) are summarized. Findings of this study and the ongoing compatibility analysis of the vertical GMMs with the updated dataset will be combined to provide a complete framework of ground motion characterization for vertical ground motion component in Turkey.

2. EXTENDING THE TURKISH STRONG GROUND MOTION DATABASE (TSMD)

AFAD's Strong Motion Database of Turkey contains 479 earthquakes with moment magnitudes bigger than 3 (M_w > 3) that occurred between years of 2008 and 2015. All recordings from these earthquakes are gathered; however, events or records with following characteristics are eliminated: (i) events with focal depths more than 30 km, (ii) events with M_w < 3.5, (iii) events with unknown style-of-faulting, (iv) records with source to site distance is greater than 200 km, (v) stations with unknown time-based average of shear wave velocity profile of top 30m (V_{S30}), (vi) events with less than three recordings. After the preliminary elimination, 1189 records from 162 earthquakes are compiled and added to TSMD. Additionally, 268 recordings from the recent Ayvacık earthquake swarm that satisfies the conditions above are included, leading to 1457 strong motion recordings from 184 events. The event location information (epicentral coordinates and focal depth) is obtained from AFAD's database. Magnitude values and the fault plane solutions are retrieved from Global CMT (http://www.globalcmt.org/CMTsearch.html), Regional Centroid Moment Tensor (http://rcmt2.bo.ingv.it/) and GFZ Moment Tensor (http://gfzpublic.gfz-potsdam.de) databases. No magnitude conversion equation was utilized because the majority of the recordings are from small magnitude (M<5) events. The style-of-faulting is determined by application of P- and T-axes definitions provided by Boore and Atkinson (2007) [5]. Source to site distance metrics are calculated using the procedure given in Akkar et al. (2014) [3]. Figure 1 shows the distribution of the earthquakes and records attributed to the normal, reverse and strike-slip earthquake mechanisms. Majority of the earthquakes have normal and

strike-slip mechanisms, whereas only a few reverse events are available. When the recording stations are classified in NEHRP site classes (BSSC, 2015[6]), more than 90% of the records and stations belong to class D ($180<V_{S30}<360$) and class C ($360< V_{S30}<760$) (Figure 2).

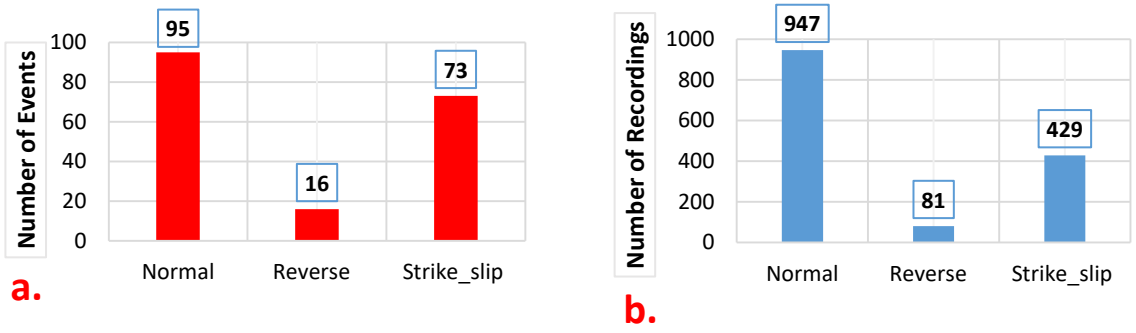

FIG. 1. (a) Number of events, (b) number of records for each style of faulting category

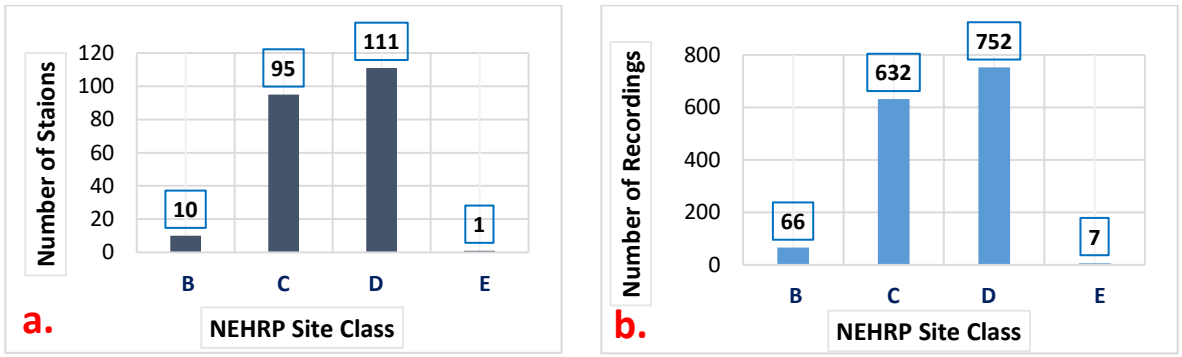

FIG. 2. (a) Number of stations, (b) number of records in each NEHRP site class.

The procedure that is employed TSMD (Akkar et al. 2010[1]) is followed in the processing of the additional recordings. Utilized processing scheme includes the visual inspection of each recording for non-standard errors (Douglas, 2003 [7]) and applying a zeroth-order correction. The low-cut (high pass) and high-cut (low-pass) filter values are determined by an iterative procedure that monitors the behavior of the Fourier amplitude spectrum as well as the velocity and displacement time series (Akkar and Boore, 2003 [8]). Low-cut filter values are selected carefully becouse they directly affect the usable spectral range and inappropriate low-cut filter values may lead to the loss of the major part of the accelerometric information. Theoretical corner frequency line (AS00 line) proposed by Atkinson and Silva (2000) [9] is used to check the selected low-cut filter values. Figure (3a) shows that all points are located below the AS00 line and the preferred low-cut filter values are in expected correlation with magnitude (please note that the majority of recorders are modern digital instruments). The maximum usable period for each recording is calculated by taking the inverse of 1.25 times the low-cut filter value. Figure (3b) shows the number of recordings as a function of maximum usable period. It is observed that the number of records reduces significantly for periods larger than 3s. The response spectra of vertical and two horizontal components are calculated and the geometric average of horizontal components are used in calculations ([10,11,12]).

When the TSMD is updated with the additional recordings defined above, the final updated dataset contains 2698 recordings from 672 earthquakes. The magnitude-distance distribution of the updated TSMD for peak ground acceleration (PGA) is given in Figure 4 (original TSMD and new recordings are represented by blue triangles and red circles, respectively). Figure 4 shows that the majority of strong ground motion recordings in the original TSMD

belonged to $5<M_w<6.5$ events recorded at distances more than 30 kilometers; therefore, near field recordings of large magnitude events which are critical from engineering design point of view were limited. Also, the number of recordings for $M_w<5$ earthquakes, which play an important role in defining the regional magnitude scaling were not sufficient (Gülerce et al., 2016 [4]; Sandıkkaya, 2017[13]). Updated TSMD includes subtantially more recordings from small magnitude events and the number of near-field recordings is improved in the moderate magnitude range.

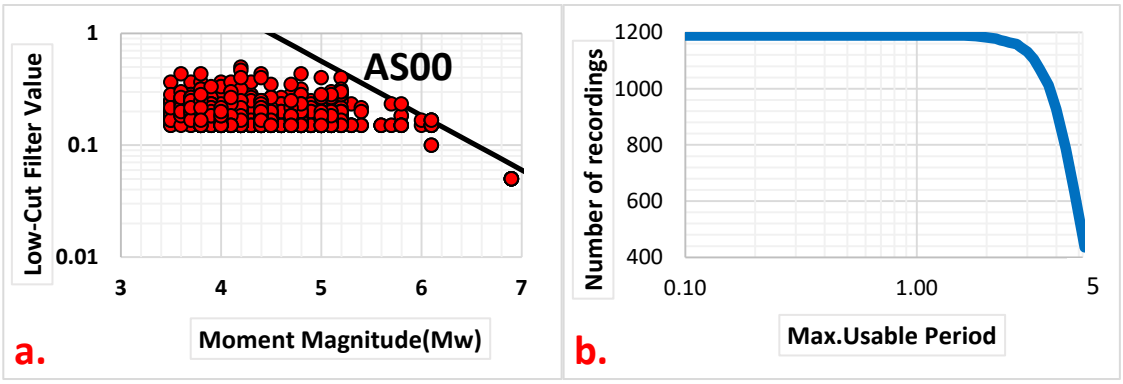

FIG. 3. (a) Distribution of low cut filter values with magnitude and comparison with the theoretical corner frequency line, (b) period dependence of number of ground motions based on the lowest useable frequency.

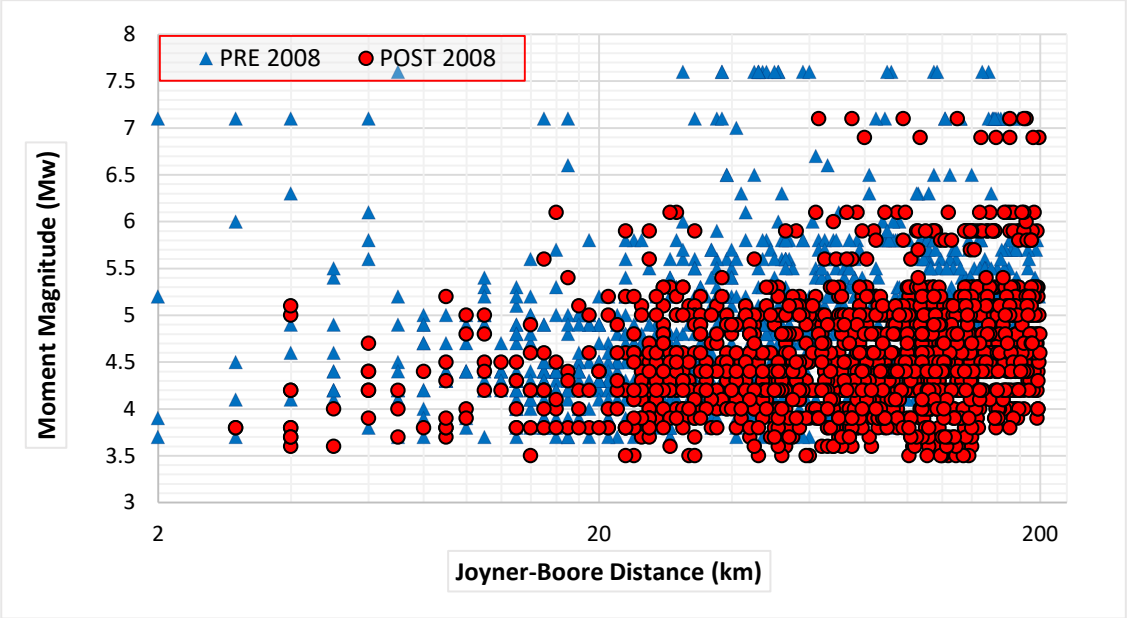

FIG. 4. Distribution of magnitude-distance pairs for PGA

3. SELECTION OF THE CANDIDATE V/H RATIO MODELS

The GMM selection criteria proposed by Cotton et al. (2006) [14], Bommer et al. (2010) [15] and Stewart et al. (2016) [16] for horizontal GMMs are utilized to select four candidate V/H ratio models in this study. Global models proposed by Gülerce and Abrahamson (2011; GA2011 [17]) and Bozorgnia and Campbell (2016; BC2016 [18]) were built using the NGA-West 1 (Chiou et al., 2008 [19]) and NGA-West 2 (Anceta et al., 2014 [20]) databases, respectively. The Akkar et al. (2014b) [21] European model was derived from the RESORCE database. Gülerce and Akyüz (2013; GA 2013 [22]) GMM is a regionalized version of

GA2011 V/H ratio model for Turkey; the functional form of the model is the same as that of GA2011 but some of the coefficients are adjusted using the original TSMD. Tables 1 and 2 summarize the main features of the candidate models in terms of applicability ranges, independent parameters, etc.

TABLE 1: FUNCTIONAL FORMS OF THE CANDIDATE V/H MODELS

Candidate GMM	**Functional Form (for median)**
GA 2011	$\ln\left(\frac{V}{H}\right) = f_{Mag,Rrup} + f_{flt} + f_{site}$
GA 2013	$\ln\left(\frac{V}{H}\right) = f^{*}_{Mag,Rrup} + f_{flt} + f^{*}_{Site}$
Akkar et al. 2014	$\ln\left(\frac{V}{H}\right) = f_{Mag,Rjb} + f_{flt} + f_{site}$
BC 2016	$\ln\left(\frac{V}{H}\right) = f_{Mag} + f_{Rrup} + f_{flt} + f_{HW} + f_{site} + f_{sed} + f_{hyp} + f_{dip} + f_{atn}$
Notes: Abbrevations used in the table are: Mag: moment magnitude, Site: site amplification, flt: faulting mechanism, Rrup: rupture distance, Rjb: Joyner-Boore distance, HW: hanging wall effect**, sed: basin response effects, hyp: hypocentral depth, dip: dip angle, atn: large distance attenuation. *Same funtional form but some of the coeffiecients are TR-adjusted. **Hanging-wall effects are neglected in our study.	

TABLE 2. PROPERTIES AND APPLICABILITY RANGES OF THE V/H MODELS

General Information				**Applicability Range**		
Candidate GMM	**Database**	**Number of recordings**	**Number of events**	**M_w range**	**Distance range (km)**	**Spectral period range (sec)**
GA 2011	PEER-NGA W1	2684	127	5-8	0-200	0-10
GA 2013	Built by PEER-NGA W1, (Modified by TSMD)	2684 (1142)	127 (288)	5-8 (4-8)	0-200	0-10
Akkar et al. 2014	RESORCE	1041	221	4-8	0-200	0.01-4
BC 2016	PEER-NGA W2	6989	282	3-8	0-300	0-10

4. ANALYSIS OF THE RESIDUALS

To evaluate the misfit between the model predictions and the actual ground motion data, median estimations of each candidate model are computed using the predictive parameters in the updated TSMD. The total residual, denoted by R_{ijk}, is the difference between the natural logarithm of the observed ground motion a_{ijk} and the model prediction, p_{ijk} from the i^{th} event

at the j^{th} station at period k (Eq. 1). Then, using the the random effects regression (Abrahamson and Youngs, 1992 [23]), the total residuals are decomposed into three components: the mean offset (c_k) representing the average bias of the actual data relative to the model predictions in each period, between-event ($\emptyset_{jk}$) and within-event (τ_{jik}) residuals (e.g. Scassera et al., 2009 [24], Al-Atik et al. (2010) [25]).

$$R_{ijk} = \ln(a_{ijk}) - \ln(p_{ijk}) = c_k + \phi_{jk} + \tau_{ijk} \qquad (1)$$

To check the compatibility of the magnitude and depth to the top of the rupture (Z_{tor}) scaling of the candidate models with the updated TSMD, total between-event residuals ($c_k + \emptyset_{jk}$) are plotted with respect to M_w and Z_{tor} for PGA, T = 0.07s, 0.3s, and 1.0s spectral accelerations in Figures 6-9, respectively. The analysis were performed for several other spectral periods but these periods are presented since they approximately represent the positive and negative peaks of the V/H ratio. In each figure, the total between-event residuals for strike-slip, reverse and normal events are given by red, black and green symbols; whereas, the average of the residuals is shown by pink lines. Similarly, the distribution of the within-event residuals with record parameters such as distance and V_{S30} is given in Figures 6-9.

Three candidate models, GA2013, Akkar et al. (2014), and BC2016 show similar trends in the residuals vs. magnitude plots. Average residuals of these models are generally positive for small magnitudes, especially for M_w <4 events. The average residuals lie very close to the zero line, especially after 0.3s. On the other hand, GA2011 V/H model underestimates the observed ground motions for periods upto 0.5s. and overestimates after T=1s., especially for M_w <6.5 events. Even if the functional form is the same, magnitude scaling of GA2013 model has a better fit with the observed data when compared to GA2011. This observation can be explained by the modification of the GA2011 model's constant term based on the mean offset in residuals of original TSMD. Distribution of the total between-event residuals imply that the Z_{tor} scaling of all models are consistent with the updated TSMD; no linear trends are observed for Z_{tor}<20km except for a small constant shift.

Distribution of intra-event residuals with distance suggests no trends within the applicability range of the selected models, except for a small constant shift observed in the GA2011 model residuals. Performance of GA2013, Akkar et al. (2014) and BC2016 models in site amplification scaling are equally good; no trends are observed in the distribution of intra-event residuals with V_{S30}. It is notable that the correction applied to the site amplification term of GA2011 by Gülerce and Akyüz (2013) significantly improved constant shift observed in the residuals of GA2011. Amount of reverse events and recordings from these events in the updated TSMD are limited; however, the distribution of the residuals with any of the seismological parameters does not show a significant variation with style-of-faulting.

The mean offset values (c_k) for the candidate GMMs are compared in Figure 10 to observe the general tendency in the model performances. The mean offsets of GA2013, Akkar et al. (2014), and BC2016 models are close to each other; however, the average misfit along the periods is minimum for Akkar et al. (2014) model, closely followed by BC2016 and GA2013 models. The maximum misfit is obtained for the GA2011 model, consistent with the observations from the residual plots.

5. CONCLUSIONS

The preliminary objective of this study was to update the original TSMD since siginificant amount of data in small-to-moderate magnitude range has obtained after the earthquakes occurred after 2008. 1457 recordings from 184 events after 2008 were selected and analyzed.

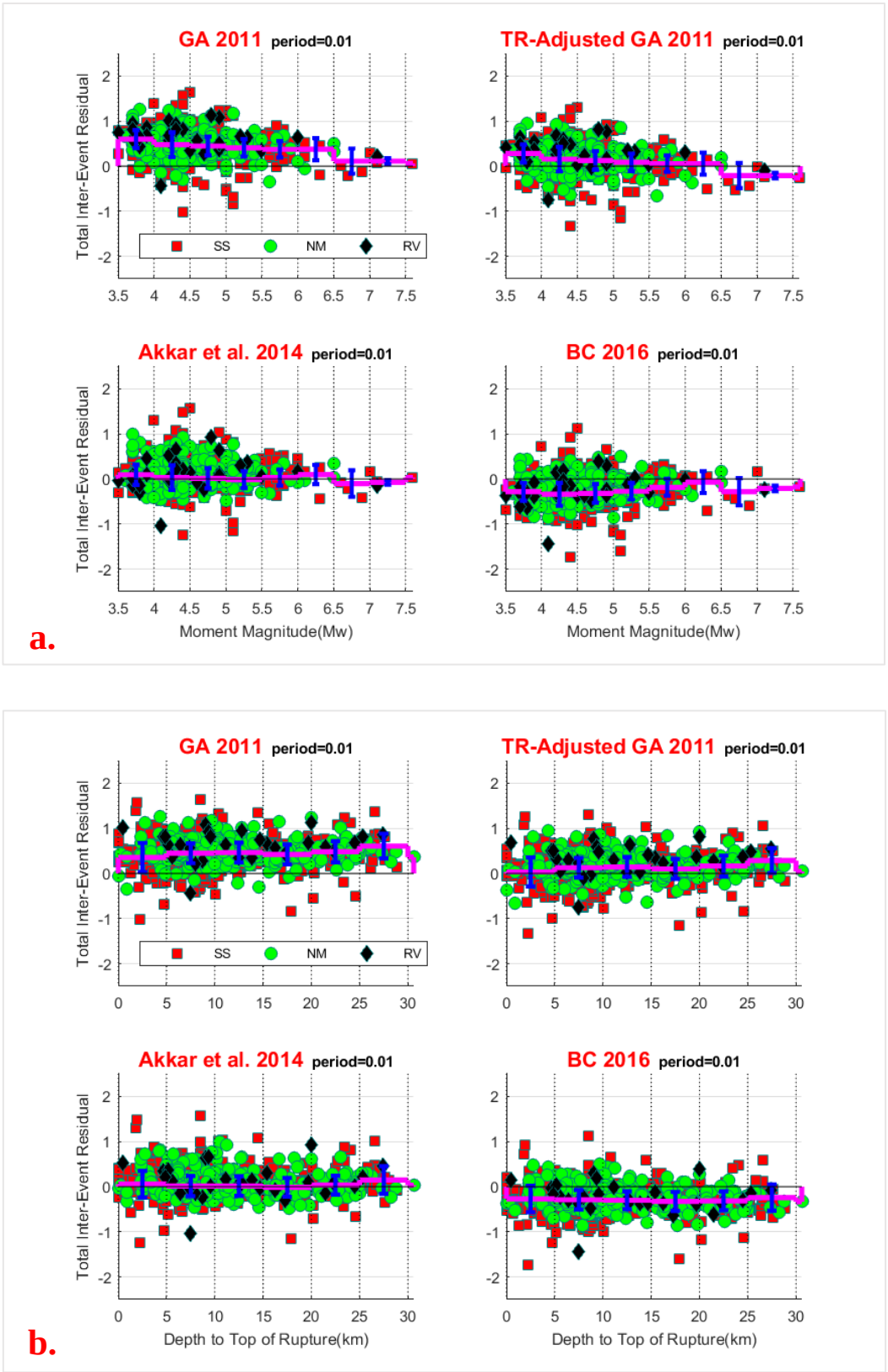

FIG. 6. Distribution of the total inter-event residuals with (a) magnitude, (b) depth to the top of the rupture for Sa at 0.01sec or at PGA depending on the model.

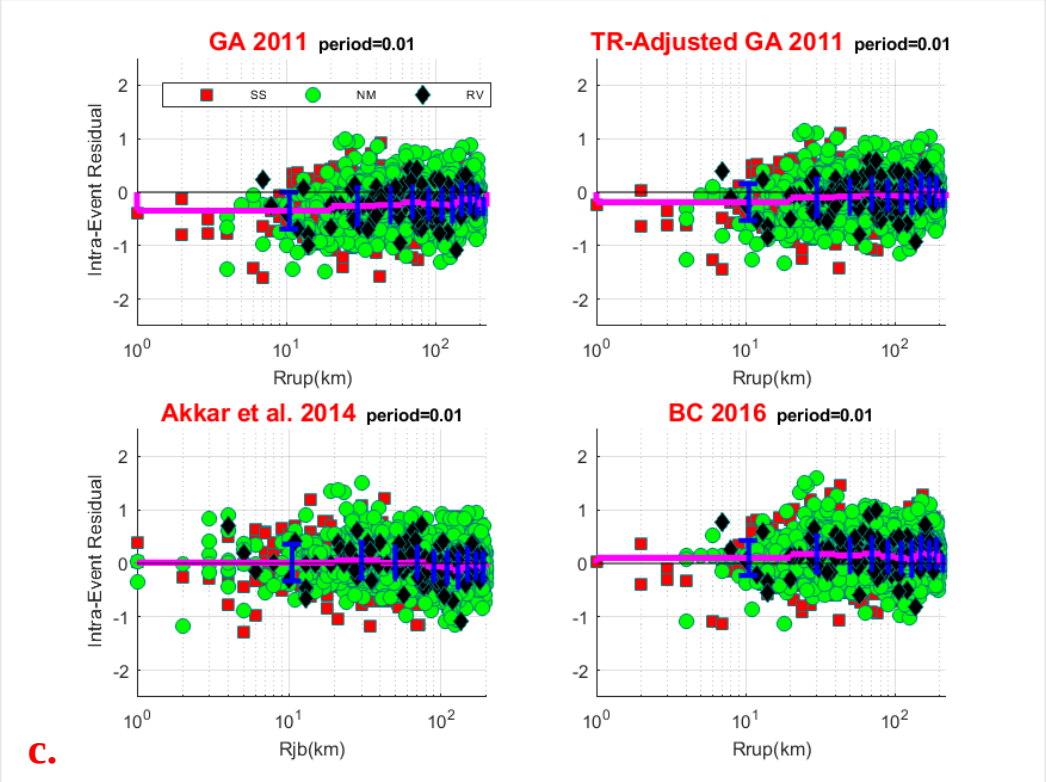

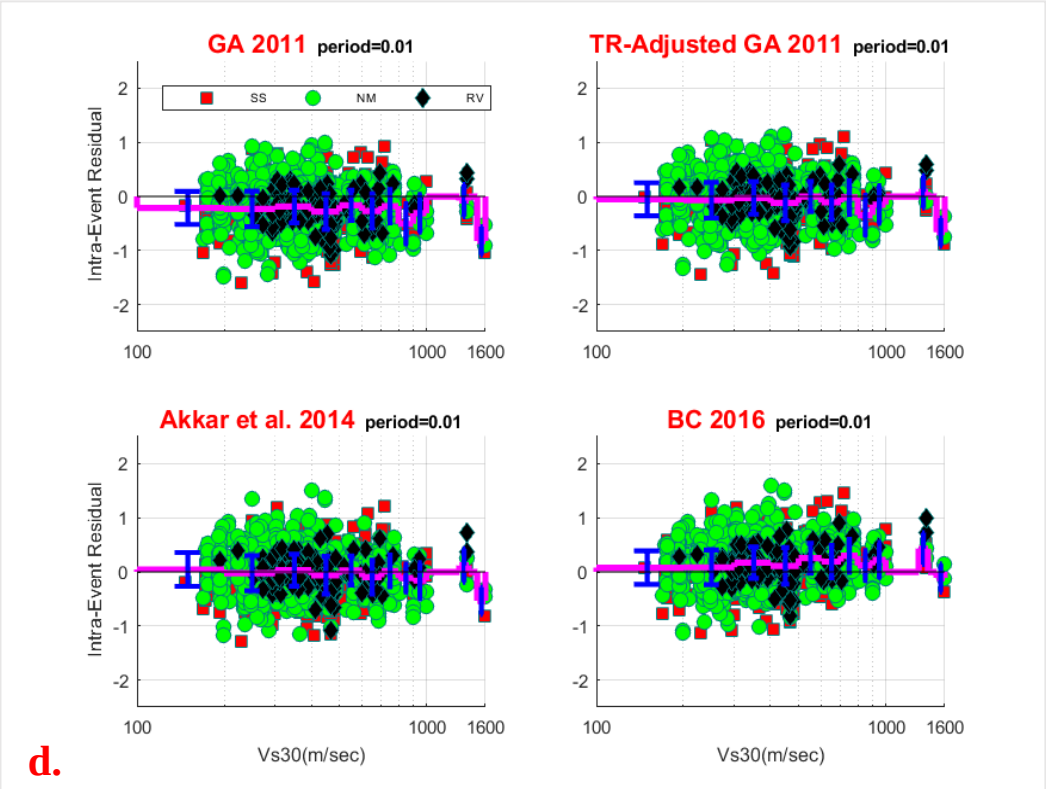

FIG. 6 (continued). Distribution of the intra-event residuals with (a) rupture distance or Joyner-Boore distance depending on the model, (b) V_{S30} for Sa at 0.01sec or at PGA depending on the model.

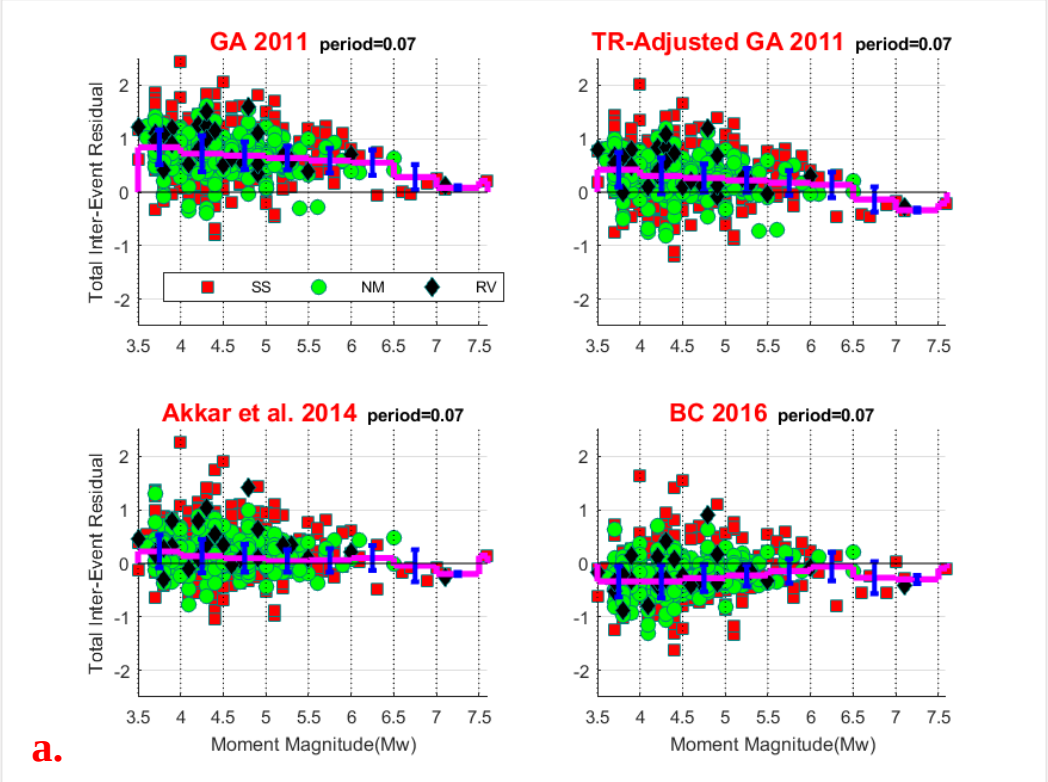

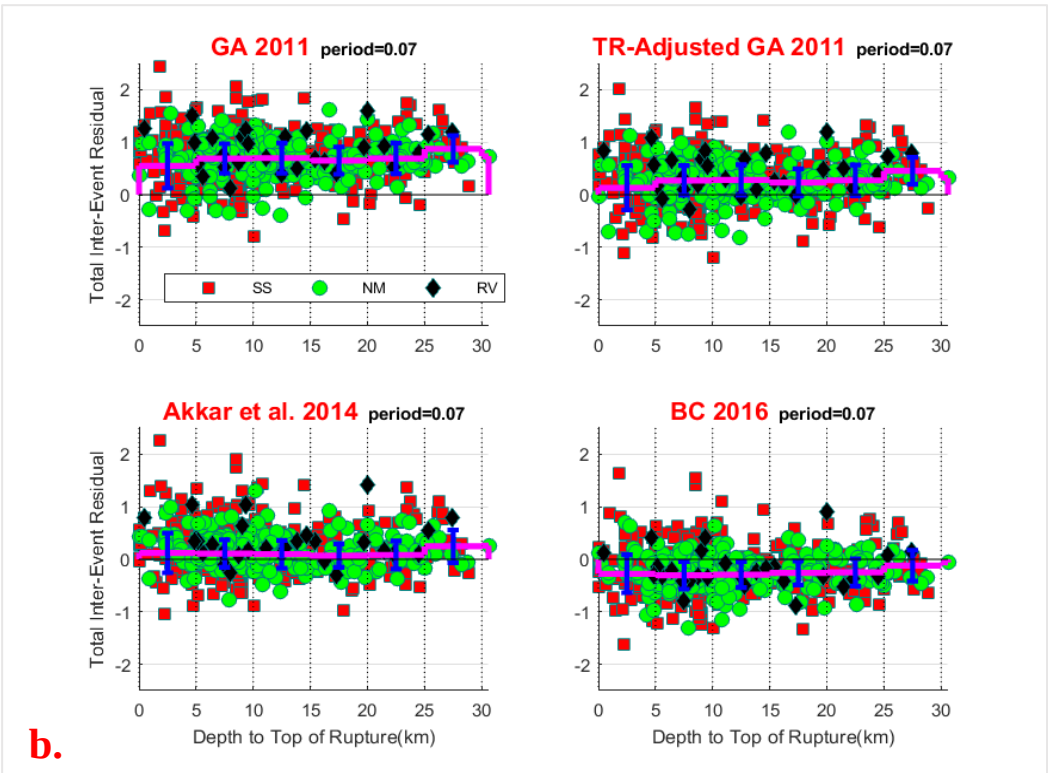

FIG. 7. Distribution of the total inter-event residuals with (a) magnitude, (b) depth to the top of the rupture for Sa at 0.07sec.

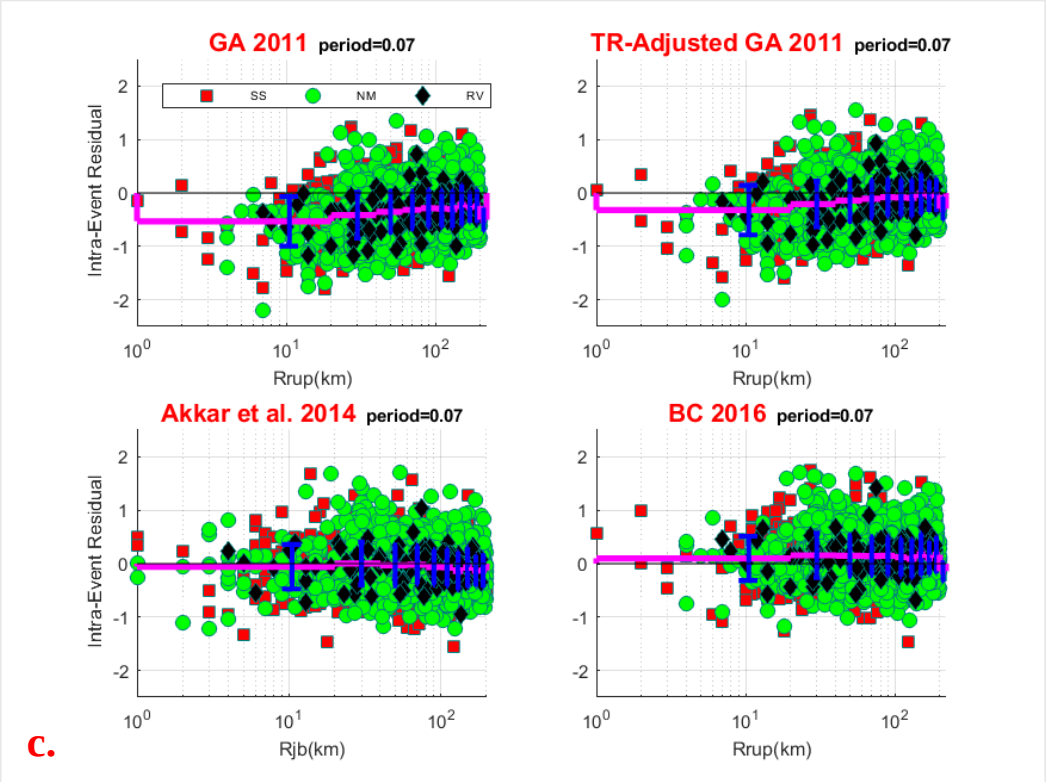

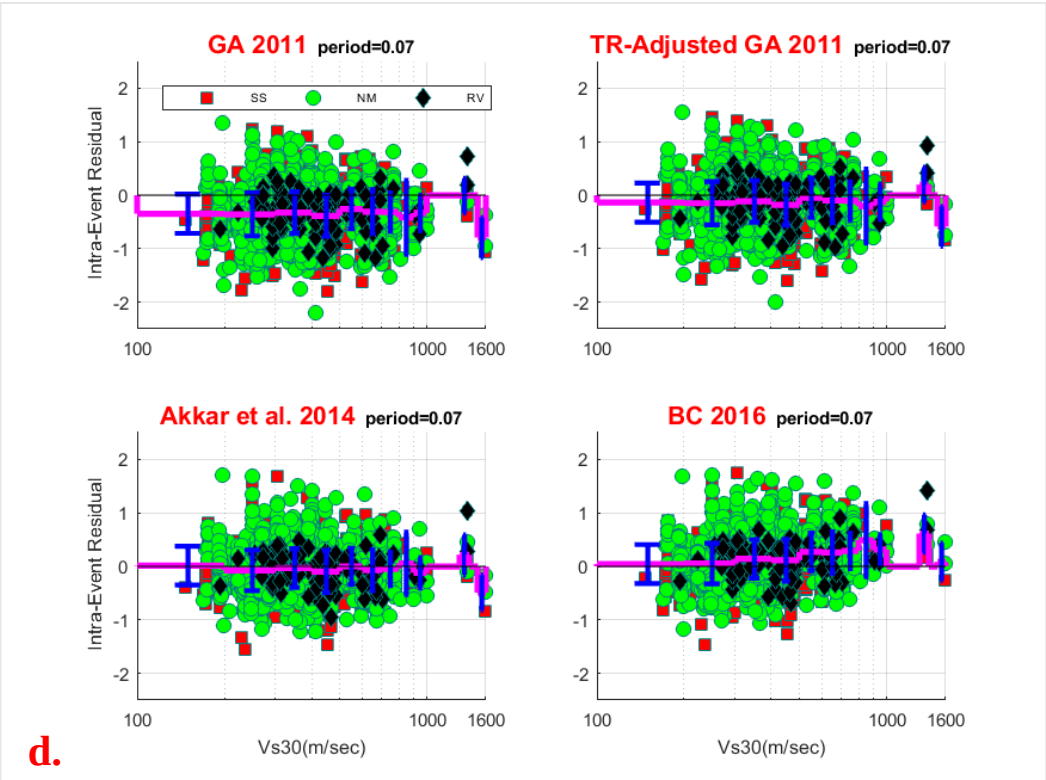

FIG. 7 (continued). Distribution of the intra-event residuals with (a) rupture distance or Joyner-Boore distance depending on the model, (b) V_{S30} for Sa at 0.07sec.

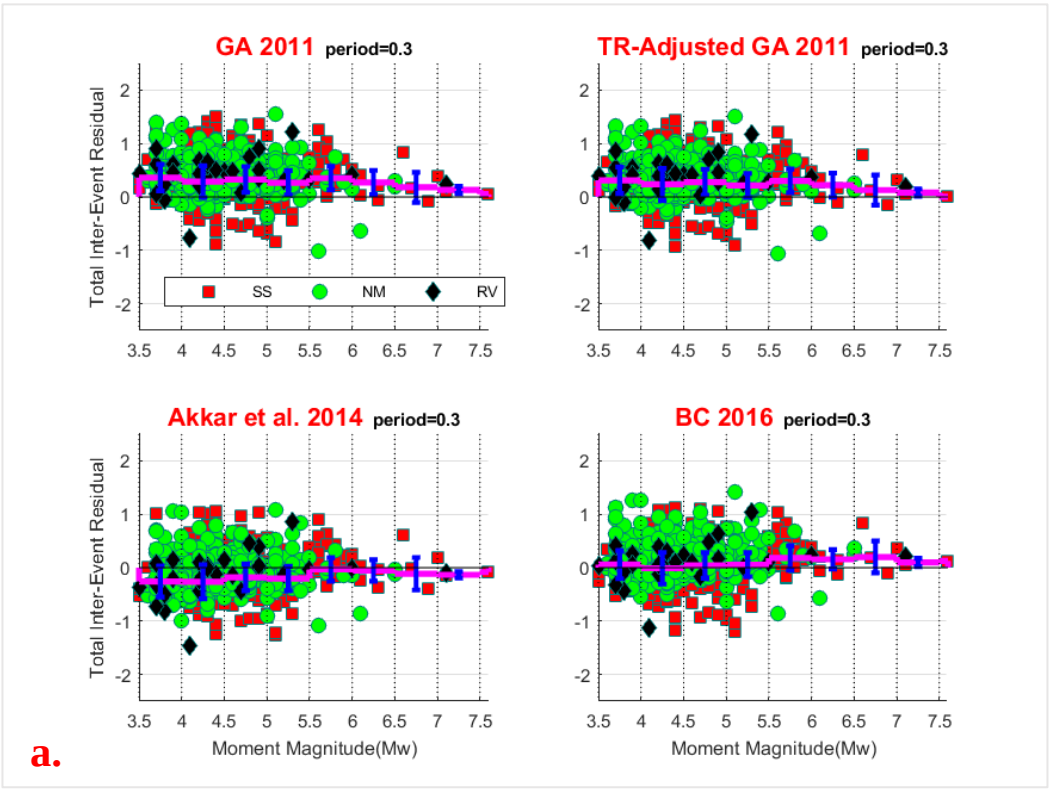

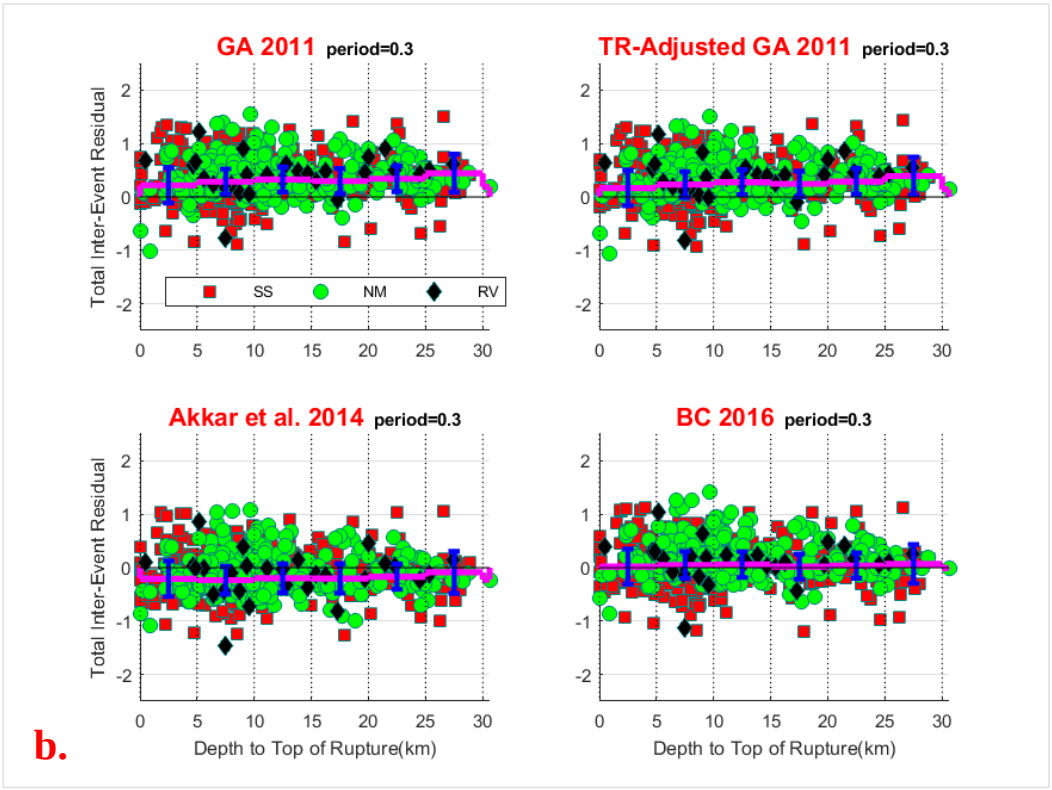

FIG. 8. Distribution of the total inter-event residuals with (a) magnitude, (b) depth to the top of the rupture for Sa at 0.3 sec.

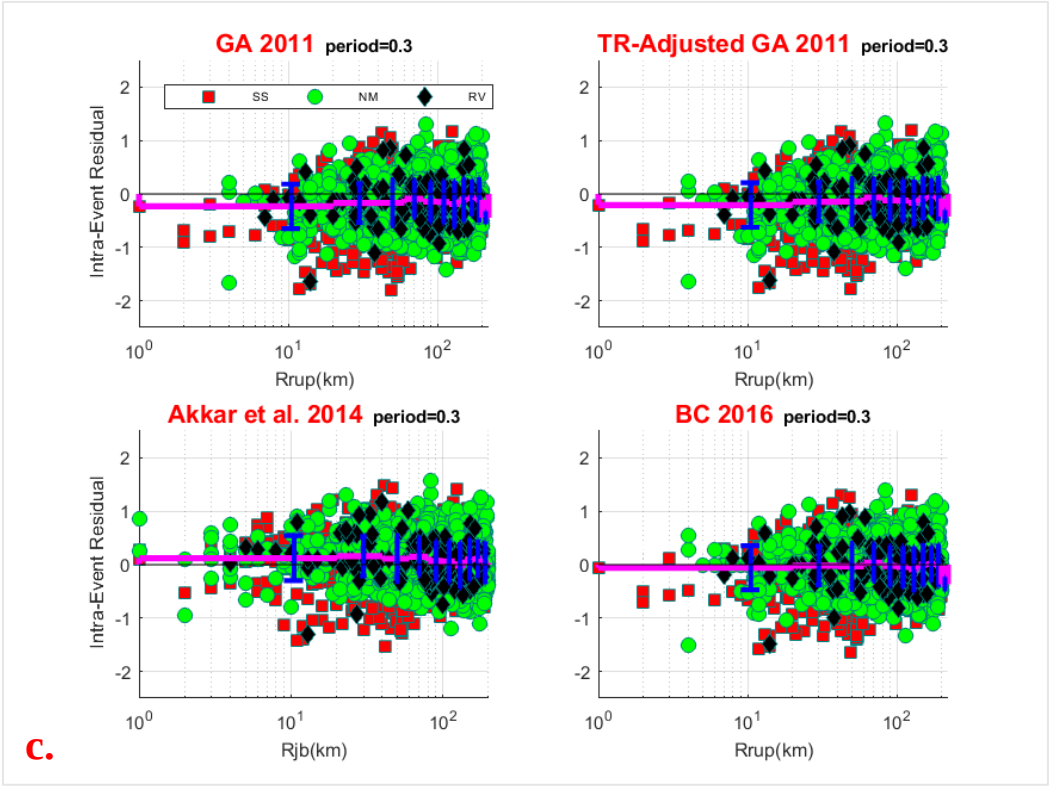

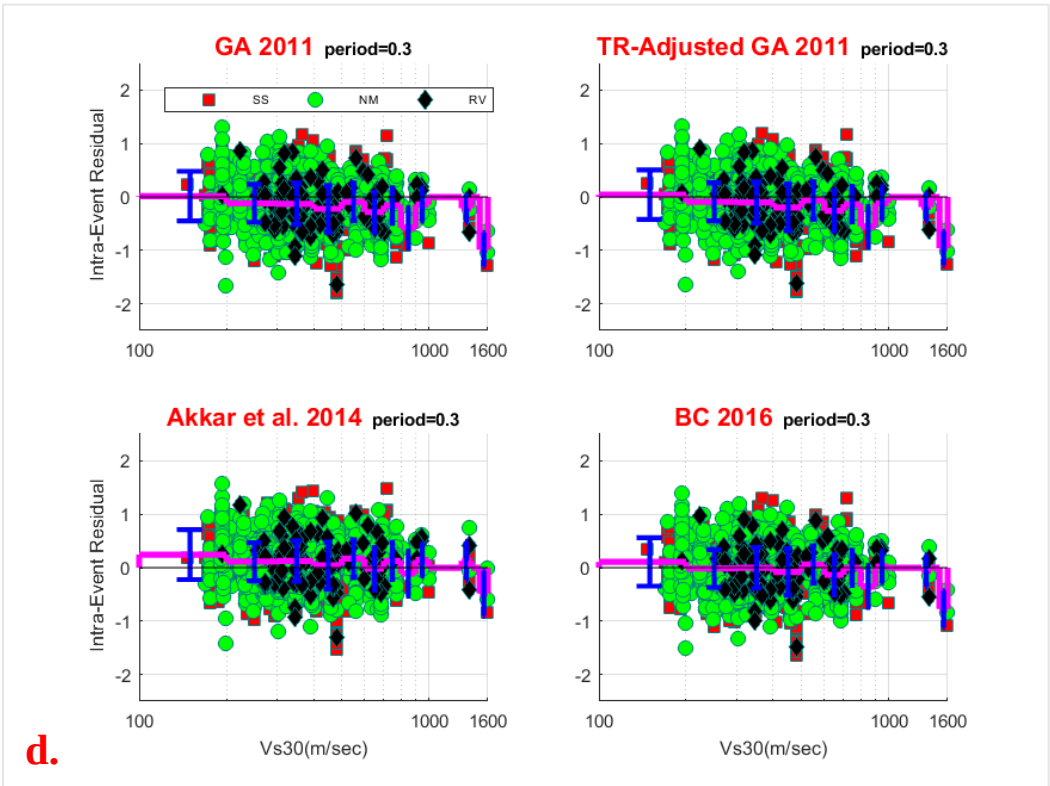

FIG. 8 (continued). Distribution of the intra-event residuals with (a) rupture distance or Joyner-Boore distance depending on the model, (b) V_{S30} for Sa at 0.3 sec.

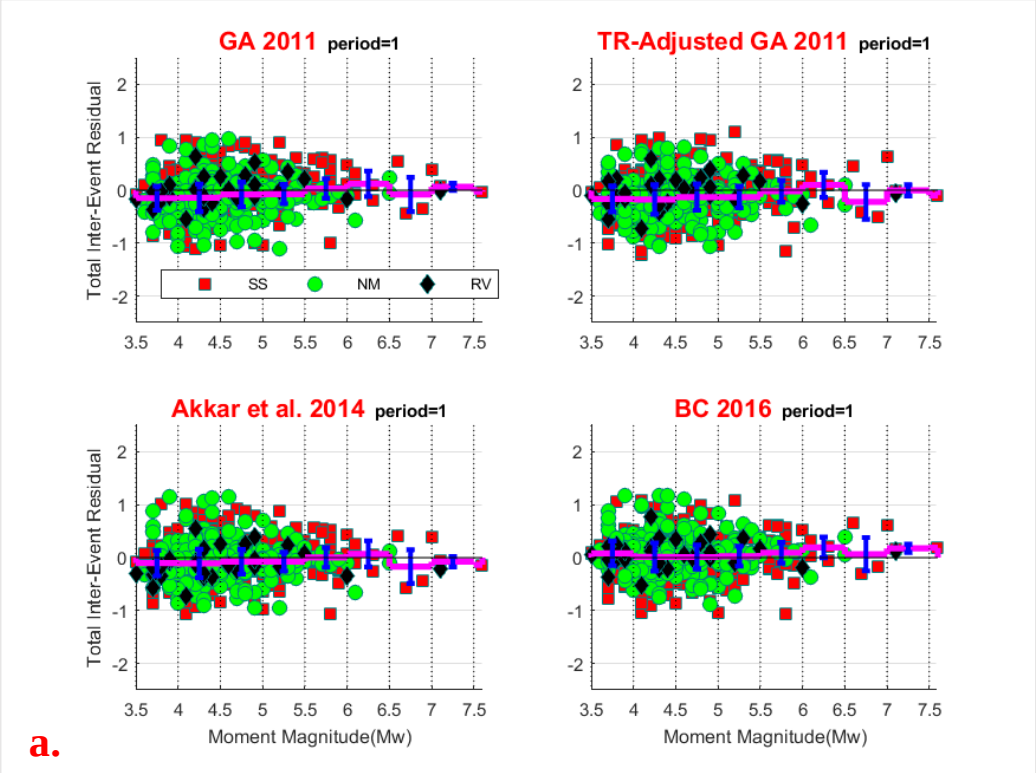

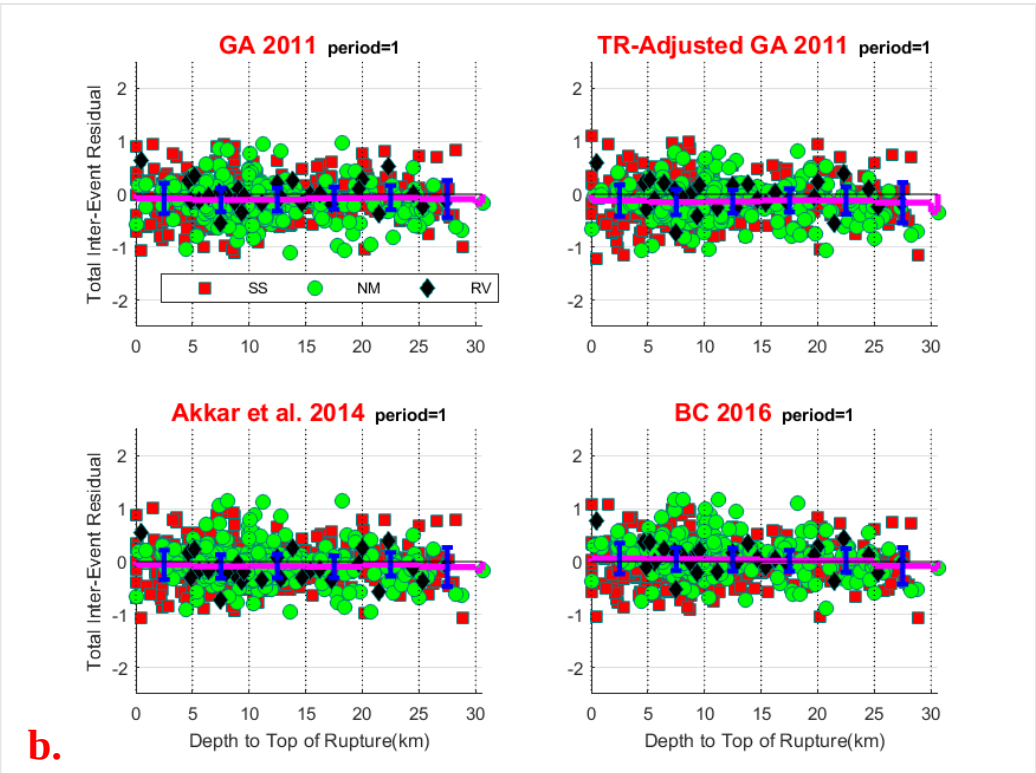

FIG. 9. Distribution of the total inter-event residuals with (a) magnitude, (b) depth to the top of the rupture for Sa at 1 sec.

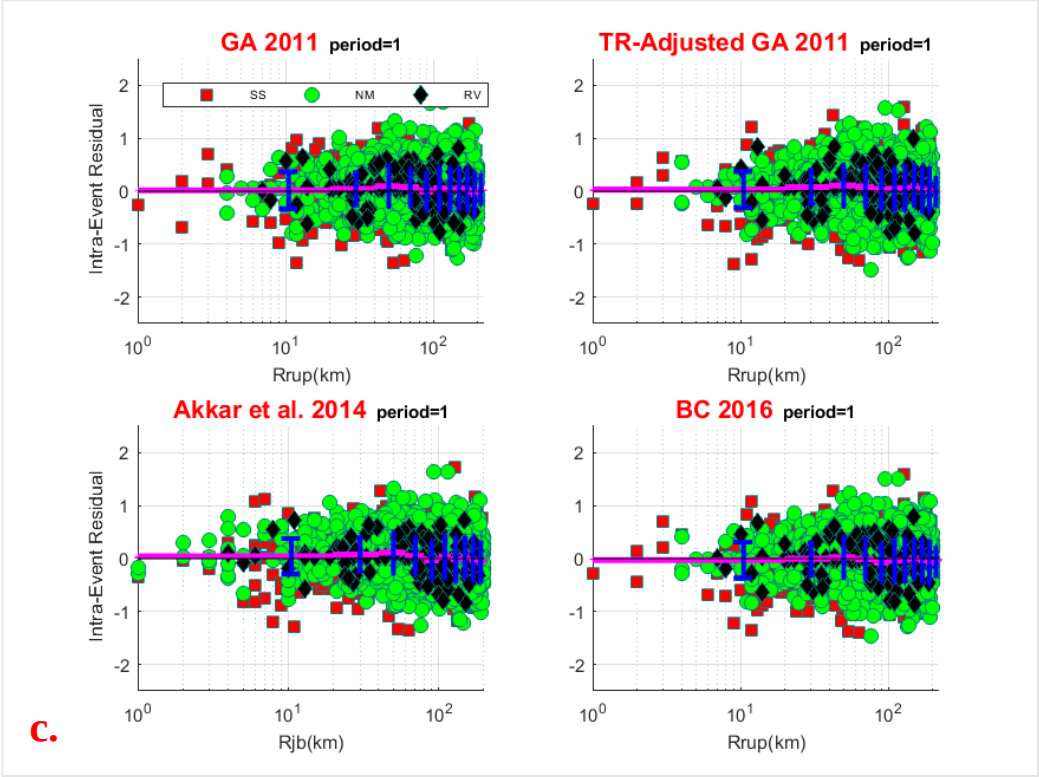

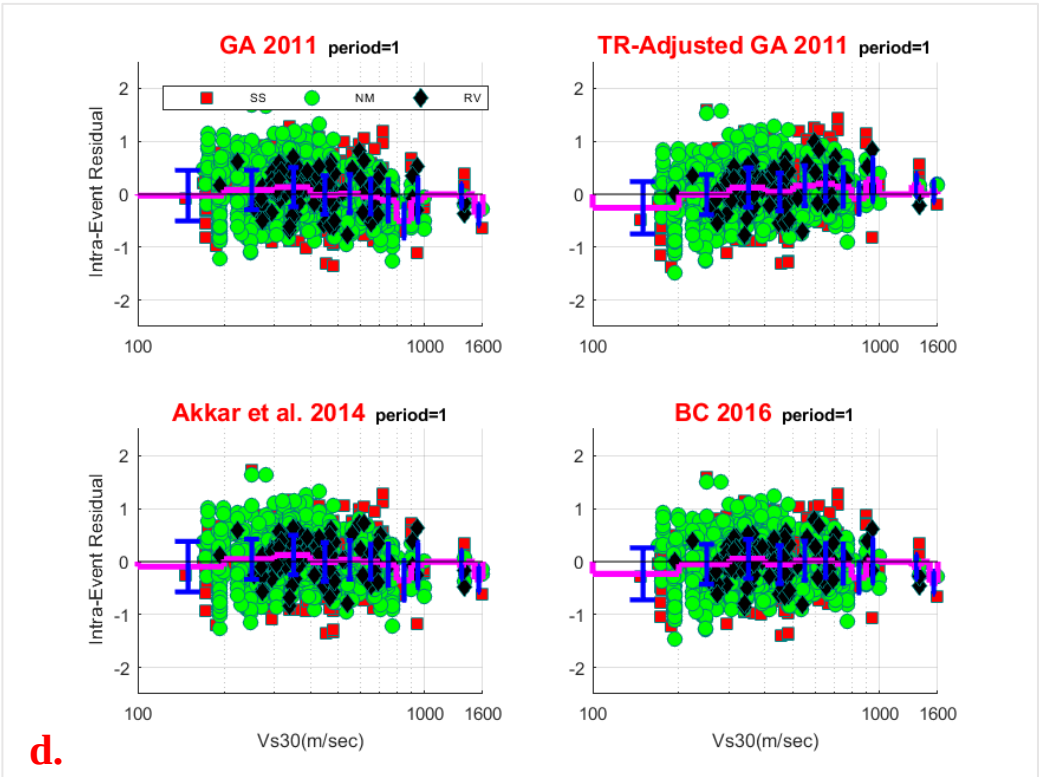

FIG. 9 (continued). Distribution of the intra-event residuals with (a) rupture distance or Joyner-Boore distance depending on the model, (b) V_{S30} for Sa at 1 sec.

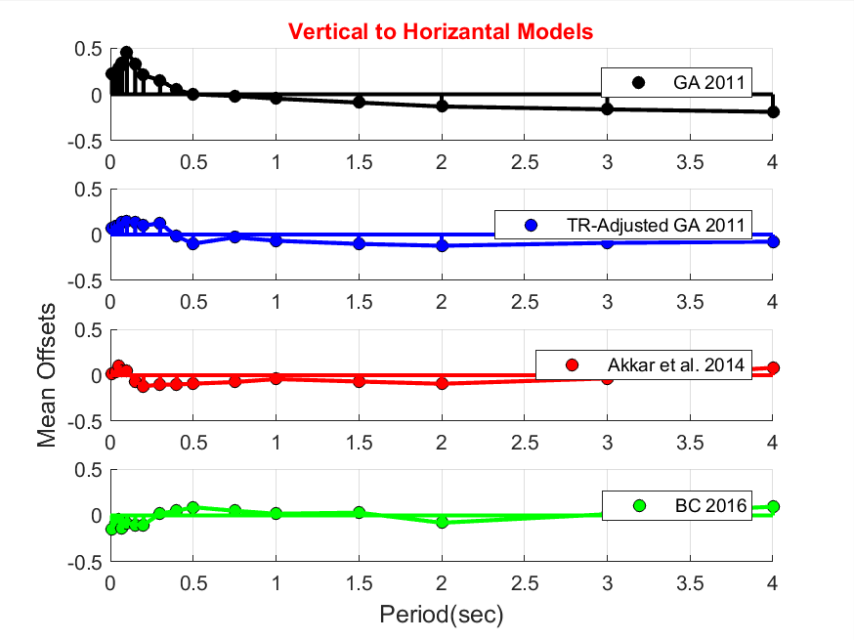

FIG. 10. Distribution of mean offsets for each candidate model.

These recordings were added to the original TSMD after a processing procedure consistent with the TSMD is applied. Updating the TSMD significantly increased the number of data in the original version, especially in the moderate magnitude range; therefore, the updated TSMD is suitable for testing the applicability of GMMs for PSHA studies in Turkey. The main objective of the study was to propose a framework for developing the site-specific vertical design spectrum using PSHA outputs. The vertical ground motions are frequently calculated based on V/H ratio GMMs, therefore, four candidate V/H ratio models were selected and their compatibility with the updated TSMD in terms of magnitude, distance, and site effects were evaluated using the analysis of residuals. Analysis results showed that the GA2013, Akkar et al. (2014), and BC2016 GMMs are suitable for ground motion characterization studies in Turkey for the vertical ground motion component. Akkar et al. (2014) GMM does not require any modification for Turkey; whereas the constant terms of GA2013 and BC2016 GMMs may be adjusted based on the updated TSMD.

REFERENCES

[1] S. AKKAR, Z.ÇAĞNAN, E.YENİER, Ö. ERDOĞAN, M.A.SANDIKKAYA, P. GÜLKAN., "The recently compiled Turkish strong motion database: preliminary investigation for seismological parameters ", Journal of Seis. 14.3 (2010): 457-479.

[2] M.A.SANDIKKAYA, M.T.YİLMAZ, B.S.BAKİR, Ö. YILMAZ., " Site classification of Turkish national strong-motion stations", Journal of Seismology 14.3 (2010): 543-563.

[3] S. AKKAR, et al., "Reference database for seismic ground-motion in Europe (RESORCE)", Bulletin of Earthquake Engineering 12.1 (2014): 311-339.

[4] Z.GÜLERCE, B. KARGIOĞLU, N.A. ABRAHAMSON., "Turkey-Adjusted Next Generation Attenuation West-1 Models for Horizontal Ground Motions ", Earthquake Spectra 32.1 (2016): 75-100.

[5] D.M. BOORE, G. M.ATKINSON., "Boore–Atkinson NGA ground motion relations for the geometric mean horizontal component of peak and spectral ground motion parameters", Pacific Earthquake Engineering Research Center, 2007.

[6] NATIONAL EARTHQUAKE HAZARD REDUCTION PROGRAM (NEHRP), Building Seismic Safety Council (BSSC 2015).

[7] J.DOUGLAS., "What is poor quality strong-motion record?", Bulletin of Earthquake Engineering 1.1 (2003): 141-156.

[8] D.M.BOORE, S. AKKAR., "Effect of causal and acausal filters on elastic and inelastic response spectra", Earthquake Eng. & Structural Dynamics 32.11 (2003): 1729-1748.

[9] GM.ATKINSON, W.SILVA., "Stochastic modeling of California ground motions", Bulletin of the Seismological Society of America 90.2 (2000): 255-274.

[10] S. AKKAR, J.J.BOMMER., "Influence of long-period filter cut-off on elastic spectral displacements", Earthquake Engineering & Structural Dynamics 35.9 (2006): 1145-1165.

[11] D.M.BOORE, J.J.BOMMER., "Processing of strong-motion accelerograms? Needs, options and consequences", Soil Dynamics and Earthquake Eng. 25.2 (2005): 93-115.

[12] J.DOUGLAS, D.M.BOORE., "High-frequency filtering of strong-motion records", Bulletin of Earthquake Engineering 9.2 (2011): 395-409.

[13] M.A.SANDIKKAYA., "Effects of Low Magnitude Records on Ground-Motion Prediction Equations", Journal of Earth Sciences 37.3 (2017): 237-252 .

[14] F.COTTON, F. SCHERBAUM, J.J.BOMMER, H.BUNGUM., "Criteria for selecting and adjusting ground-motion models for specifc target regions: application to Central Europe and rock sites", Journal of Seismology 10.2 (2006): 137.

[15] J.J.BOMMER, et al., "On the selection of ground-motion prediction equations for seismic hazard analysis", Seismological Research Letters 81.5 (2010): 783-793.

[16] JP.STEWART, et al., "Selection of ground motion prediction equations for the Global Earthquake Model", Earthquake Spectra 31.1 (2015): 19-45.

[17] Z.GÜLERCE, N.A.ABRAHAMSON., "Site-Specific Design Spectra for Vertical Ground Motion", Spectra 27.4 (2011): 1023-1047.

[18] Y.BOZORGNIA, K.W.CAMPBELL., "Ground Motion Model for the Vertical-to-Horizontal (V/H) Ratios of PGA, PGV, and Response Spectra", Earthquake Spectra 32.2 (2016): 951-978.

[19] B.S.-J.CHİOU, R.R.YOUNGS., "An NGA Model for the Average Horizontal Component of Peak Ground Motion and Response Spectra", Earth. Spectra 24 (2008): 173-215.

[20] T.D.ANCHETA, et al., "NGA-West2 Database", Earth. Spectra 30 (2014): 989-1005.

[21] S. AKKAR, M.A.SANDIKKAYA, B.Ö. AY., "Compatible ground-motion prediction equations for damping scaling factors and vertical-to-horizontal spectral amplitude ratios for the broader Europe region", Bulletin of Earthquake Engineering 12.1 (2014): 517-547.

[22] Z.GÜLERCE, E. AKYÜZ., "The NGA-W1 Vertical-to-Horizontal Spectral Acceleration Ratio Prediction Equations Adjusted for Turkey", Seismological Research Letters 84.4 (2013): 678-687.

[23] N.A.ABRAHAMSON, R.R.YOUNGS., "A stable algorithm for regression analyses using the random effects model", Bulletin of the Seis. Soc. of America 82.1 (1992): 505-510.

[24] G. SCASSERA, et al., "A comparison of NGA ground-motion prediction equations to Italian data", Bulletin of the Seismological Society of America 99.5 (2009): 2961-2978.

[25] L.A.ATİK, et al., "The Variability of Ground-Motion Prediction Models and Its Components ", Seismological Research Letters 81.5 (2010): 794-801.